The Kidder Equation: $u_{xx} + 2xu_x/\sqrt{1-\alpha u} = 0$

By Roberto Iacono and John P. Boyd

The Kidder problem is $u_{xx} + 2x(1-\alpha u)^{-1/2}u_x = 0$ with $u(0) = 1$ and $u(\infty) = 0$ where $\alpha \in [0, 1]$. This looks challenging because of the square root singularity. We prove, however, that $|u(x;\alpha) - \text{erfc}(x)| \leq 0.046$ for all x, α. Other very simple but very accurate curve fits and bounds are given in the text; $|u(x;\alpha) - \text{erfc}(x + 0.15076x/(1 + 1.55607x^2))| \leq 0.0019$. Maple code for a rational Chebyshev pseudospectral method is given as a table. Convergence is geometric until the coefficients are $O(10^{-12})$ when the coefficients $a_n \sim \text{constant}/n^{-6}$. An initial-value problem is obtained if $u_x(0, \alpha)$ is known; the slope Chebyshev series has only a fourth-order rate of convergence until a simple change-of-coordinate restores a geometric rate of convergence, empirically proportional to $\exp(-n/8)$. Kidder's perturbation theory (in powers of α) is much inferior to a delta-expansion given here for the first time. A quadratic-over-quadratic Padé approximant in the exponentially mapped coordinate $z = \text{erf}(z)$ predicts the slope at the origin very accurately up to about $\alpha \approx 0.8$. Finally, it is shown that the singular case $u(x;\alpha = 1)$ can be expressed in terms of the solution to the Blasius equation.

1. Introduction

Kidder showed nearly 60 years ago that flow through a porous medium could be modeled by the solution of the nonlinear ordinary differential equation (ODE) on a semi-infinite interval [24]

$$u_{xx} + 2x\frac{1}{\sqrt{1-\alpha u}}u_x = 0, \qquad u(0) = 1, u(\infty) = 0, \qquad (1)$$

Address for correspondence: John P. Boyd, Department of Atmospheric, Oceanic, and Space Science, University of Michigan, 2455 Hayward Avenue, Ann Arbor MI 48109, USA; e-mail: jpboyd@umich.edu

where the parameter $\alpha \in [0, 1]$. Kidder himself observed that for $\alpha = 0$, the exact solution is

$$u_0 = 1 - \text{erf}(x) \equiv \text{erfc}(x), \tag{2}$$

where $\text{erf}(x) = (2/\sqrt{\pi}) \int_0^x \exp(-y^2) dy$ is the usual error function and $\text{erfc}(x)$ is the complementary error function. $\text{Erfc}(x)$ is a decent approximation to $u(x; \alpha)$ over the whole parameter range; the maximum error is for $\alpha = 1$ where

$$\max_{x \in [0, \infty]} |u - u_0| = 0.046. \tag{3}$$

He calculated a power series in the parameter α to second order where the $O(\alpha)$ term is

$$u_1 = -\frac{1}{2\pi} \left\{ u_0 \left[1 + \sqrt{\pi} x \exp(-x^2) \right] - \exp(-2x^2) \right\} \tag{4}$$

and the $O(\alpha^2)$ term is

$$u_2 = -\frac{1}{\pi} u_1 + \frac{1}{8\pi^{3/2}} x \exp(-3x^2) - \frac{1}{2\pi} u_0 - \frac{1}{16\pi^{1/2}} x(5 - 2x^2) \exp(-x^2)[u_0]^2$$

$$+ \frac{1}{4\pi} (2 - x^2) \exp(-2x^2) u_0 + \frac{3\sqrt{3}}{16\pi} \left\{ \text{erf}(\sqrt{3}x) - \text{erf}(x) \right\}. \tag{5}$$

In his classic book on nonlinear differential equations, Davis discusses the Kidder equation and gives a table of u_0, u_1, and u_2 on pages 410–411 [16].

There have been a number of numerical and analytical studies because Agarwal and O'Regan proved existence theorems, specifically using Kidder's equation as an example [3]. Countryman and Kannan [15] proved that the solution in enclosed by a pair of explicit analytic functions:

$$\text{erfc} \left(\frac{1}{(1 - \alpha)^{1/4}} x \right) \leq u(x) \leq \text{erfc}(x). \tag{6}$$

Wazwaz [34, 35] applied the Adomian decomposition method, but his results are awful; his best prediction for $u_x(0; \alpha = 1/2)$ is -1.025 versus the true value of -1.1917. Noor and Mohyud-Din used He's homotopy/variational iteration method [26], but obtained the same incorrect slope numbers as Wazwaz.

Parand et al. applied a pseudospectral method with a rational Chebyshev basis and also with a basis of modified generalized Laguerre functions [28, 29]. Taghavi et al. also employed generalized Laguerre functions, but in a nodal or Lagrangian basis [33]. Rezaei et al. applied a pseudospectral method with a rational Legendre basis and also a sinc ("Whittaker cardinal") basis [30]. Khan et al. used a Laplace decomposition method combined with Padé approximants [23]. Abbasbandy's table 1 shows that all these authors obtained incorrect results, too [1]. Only Rezaei et al. carried their computations

Table 1

Maple Code to Compute $u(x, \alpha)$

```
# diff(u,x,x) + (2*x/(sqrt(1-alpha*u)))*diff(u,x)=0;
# u(0)=1 u(oo)=0;
restart; L:=1/2; # map parameter;
N:=200; # number of collocation points and basis functions;
Digits:=32; # number of Digits of floating point precision;
# Matlab accuracy is Digits=16;
itermax:= 5; # number of Newton iterations;
alpha:=1; # Kidder eq parameter;
with(LinearAlgebra); resida:= Vector(N,orientation=column):
u:= Vector(N,orientation=column): xa:= Vector(N,orientation=column):
a:= Vector(N,orientation=column,fill=0): Jacobian:= Matrix(N,N):
D0Matrix:= Matrix(N,N): D1Matrix:= Matrix(N,N): D2Matrix:=
Matrix(N,N):
for ii from 1 by 1 to N do ta[ii]:= evalf( Pi*(2*ii-1)/(2*N) ); tt:=ta[ii];
xa[ii]:= evalf( L*cot(tt/2)**2 ); # collocation points;
uK[ii]:= evalf( 1 -erf(xa[ii]) ); # uK= exact u(x; alpha=0);
uKx[ii]:= evalf( - 2*exp(-xa[ii]**2)/sqrt(Pi) );
uKxx[ii]:= evalf( -2*xa[ii]*uKx[ii] );
for j from 1 by 1 to N do t:=ta[ii]; cplus:= evalf(cos((j+1)*tt));
cminus:= evalf(cos((j-1)*tt));
TL:= cplus-cminus; PT:= evalf( - (j+1)*sin((j+1)*tt) + (j-1)*sin((j-1)*tt) );
PTT:= evalf( -(j+1)*(j+1)*cplus + (j-1)*(j-1)*cminus);
S := evalf(sin(tt/2)); C := evalf(cos(tt/2));
TLx:= evalf( - S * S * S * PT/(L * C)); # "TLx" is d/dx
{TL_(j+1)-TL_(j-1) } ;
TLxx:= evalf( (S**5)*(2*C*S*PTT+(3-2*S*S)*PT )/(L*L * C*C*C* 2) );
D0Matrix[ii,j] := TL ; D1Matrix[ii,j]:=TLx ; D2Matrix[ii,j]:= TLxx; od: od:
for iter from 1 by 1 to itermax do # begin Newton's iteration;
for ii from 1 by 1 to N do u:= uK[ii]; ux:=uKx[ii]; uxx:=uKxx[ii];
for j from 1 by 1 to N do u:= evalf(u + D0Matrix[ii,j]*a[j]);
ux:= evalf(ux + D1Matrix[ii,j]*a[j]); uxx:= evalf(uxx +
D2Matrix[ii,j]*a[j]); od:
sqf:= Re( 1/sqrt( 1 - alpha * u)); resida[ii]:= evalf( uxx + 2*xa[ii]*ux*sqf );
for j from 1 by 1 to N do
Jacobian[ii,j]:= evalf( D2Matrix[ii,j] +2*xa[ii] *sqf*D1Matrix[ii,j]
+ sqf*sqf*sqf *xa[ii] *ux *alpha* D0Matrix[ii,j] ); od: od:
delta:=LinearSolve( <Jacobian|resida>); print('delta=',delta);
```

(*Continued*)

Table 1

Continued

```
for j from 1 by 1 to N do a[j]:=evalf( a[j]-Re( delta[j]) ); od: # update
              resmax[iter]:=max(seq(abs(resida[k]),k=1..N));
                  print(iter,'residual norm=',resmax[iter]);
                  od: # end of iter loop [Newton iteration];
            with(plots); anpoints:= [ seq([j,abs(a[j])] ], j=1..N) ]:
   logplot(anpoints, style=line,title=cat("Cheb. coeffs., log-linear scales,
                        L=",convert(L,string)));
                    x:='x'; ng:=101; xmax:= 5;
       for k from 1 to ng do xg[k]:= evalf(xmax*(k-1)/ng + 1.0E-6);
   t:= evalf( 2*arccot( sqrt(xg[k]/L ) ) ); ug[k]:=evalf( 1 - erf(xg[k]) );
for j from 1 to N do ug[k]:=evalf( ug[k]+a[j]*(cos((j+1)*t) - cos((j-1)*t)));
                              od: od:
 upoints:= [seq([xg[j],ug[j] ],j=1..ng) ]: plotu:=plot(upoints, style=line):
   Kp:= plot(1 -erf(x),x=0..xmax,color=red); plots[display](plotu,Kp);
          uxatzero:=evalf( - 2/sqrt(Pi)): # calculate du/dx at x=0;
    for j from 1 to N do JJ:=(j+1); TLYplus:= -2*cos(JJ*Pi)*(JJ*JJ)/L;
          JJ:=(j-1); TLYminus:= -2*cos(JJ*Pi)*(JJ*JJ)/L;
         uxatzero:=uxatzero + a[j]*(TLYplus - TLYminus) ; od:
                      lprint('du/dx(0)=',uxatzero);
```

---

to moderately large degree, but converged, using two different methods, to $u_x(0, \alpha = 1/2) = -1.18868$, which is too small by 0.3 %. Only Abbasbandy and Maleki et al. [25] among previous authors obtained results accurate to three decimal places or better.

Because of the considerable numerical disagreements, we felt further studies would prove interesting.

2. Numerical studies

The code employs a rational Chebyshev pseudospectral method to discretize the differential equation and boundary conditions. The pseudospectral method, also known as "collocation," "discrete ordinates" [31], and "selected points," demands that when the series is substituted into the differential equation, the residual is zero at each of N "collocation" points. This gives a set of algebraic equations with spectral coefficients as the unknowns. The pseudospectral

interpolation points are

$$x_i = L \cot^2 \left(\frac{t_i}{2} \right) \qquad \leftrightarrow \qquad t_i \equiv \frac{(2i - 1)\pi}{2N} \qquad i = 1, \ldots, N. \quad (7)$$

The basis functions are the rational Chebyshev functions; these are defined to be the images of cosine functions under a change-of-coordinate [6, 10]

$$TL_n(x; L) \equiv \cos(2n \operatorname{arccot}(\sqrt{x/L}), \qquad (8)$$

where L is a user-choosable map parameter, set equal to 1/2 here. Two tricks are useful improvements over the standard method.
First, define $\mathfrak{p}(x; \alpha)$ by

$$u(x; \alpha) = \operatorname{erfc}(x) + \mathfrak{p}(x; \alpha) \qquad \leftrightarrow \qquad \mathfrak{p}(x; \alpha) \equiv u(x; \alpha) - \operatorname{erfc}(x), \quad (9)$$

because Kidder proved that $\mathfrak{p}(x; 0) \equiv 0$. Our experiments showed that

$$|\mathfrak{p}(x; \alpha)| \leq 0.046 \qquad \alpha \in [0, 1], x \in [0, \infty]. \qquad (10)$$

Thus, over the *entire parameter range*, $u(x, \alpha)$ is only a *small perturbation* of $u(x; 0)$. We therefore chose to write the numerical solution in the form of (9) so that the rational Chebyshev series is not required to approximate the whole solution, but only the perturbation $\mathfrak{p}(x; \alpha)$. This has multiple advantages. First, errors in the series approximation of $u_0(x)$ are eliminated. Second, the first guess $u \approx u_0(x)$ was sufficiently good over the whole parameter range that Newton's iteration converged to machine precision in no more than five iterations. It was not necessary to add lines of code to expand the initial approximation as a Chebyshev series, but instead one could set the initial values of the Chebyshev coefficients (of the perturbation) equal to zero. Third, the perturbation $p(x; \alpha)$ has *homogeneous* boundary conditions

$$\mathfrak{p}(0; \alpha) = \mathfrak{p}(\infty; \alpha) = 0. \qquad (11)$$

Fourth, the homogeneous boundary conditions can be built-in to the approximation by writing

$$u(x) \approx u_N \equiv \operatorname{erfc}(x) + \sum_{n=0}^{N-1} a_n \left\{ TL_{n+2}(x; L) - TL_n(x; L) \right\}. \qquad (12)$$

Heinrichs and collaborators have shown that such difference-of-two-Chebyshev bases yield discretization matrices with much better condition numbers than the standard Chebyshev or rational Chebyshev basis [22, 17]. Furthermore, it is no longer necessary to reserve rows of the pseudospectral matrix

TL coefficients for alpha=1/2 [red dashed]
and alpha=1 [solid black [N=200, L=1/2,
Digits=16]
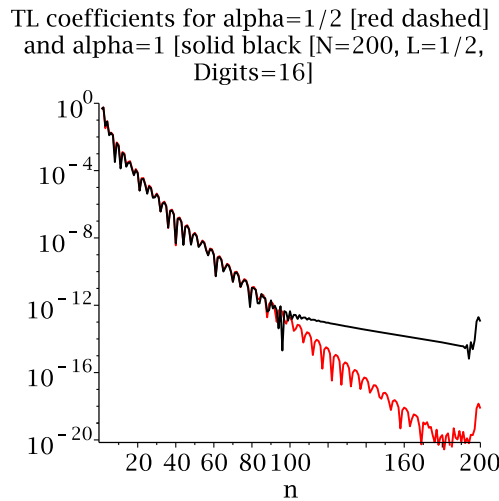
Figure 1. Absolute values of the rational Chebyshev coefficients for $u(x, \alpha = 1/2)$ [red] and $u(x, \alpha = 1)$ [solid black]. $N = 200$, map parameter $L = 1/2$ and floating point arithmetic with 16 digit precision.

to impose boundary conditions: all rows of the matrix come from collocation conditions on the differential equation, which simplifies programming.

The resulting system of algebraic equations for the coefficients of the series was solved by Newton's iteration. This requires an initialization, but as noted above, the initial guess $a_n \equiv 0$ for all n, that is, $u(x; \alpha) \approx 1 - \text{erf}(x)$ was successful without underrelaxation for the whole parameter range, $\alpha \in [0, 1]$. No more complicated strategies such as continuation-in-a-parameter was needed to generate a convergence-inducing initialization.

The rational Chebyshev algorithm, truncating the infinite series to N terms, exhibits an apparent geometric rate of convergence with respect to N over the whole parameter space except for $\alpha = 1$. The complete computer code in Maple is given in Table 1. We have avoided using Maple-specific features so that the code can be easily translated into other languages.

Despite the square root nonlinearity in the differential equation, this is a very easy problem. It is amazing that so many inaccurate results have been published.

Figure 1 shows the only anomaly. When $\alpha \neq 1$, the rational Chebyshev coefficients fall exponentially until flattening at a level controlled by floating point precision. Here, the "round-off plateau" is just above the bottom of the graph at about 10^{-19}. For $\alpha = 1$, however, the coefficient curve kinks after falling to about 10^{-12}. Such a break in form suggests that $u(x, \alpha = 1)$ is weakly singular. This is confirmed in the next section.

Table 2

Maple Code to Compute the Puiseaux Series in x about $x = 0$ when $\alpha = 1$

```
    nterms:=40; assume( y > 0, S > 0); u:= 1 - S*x;
for j from 1 to nterms do u:= u + p[j] * x**(1+j*(3/2) );
        r:=sqrt(1 - u)*diff(u,x,x) + 2*x*diff(u,x);
        rr:= subs(x=y*y,r); rrs:= series(rr,y,3*j+8);
p[j]:= solve(coeff(rrs,y,3*j-1),p[j]); od: assign(S= 1.32814);
```

3. Analysis of $\alpha = 1$

### 3.1 Branch point at the origin: Explaining the kink in the rational Chebyshev coefficients

The parameter value $\alpha = 1$ is special because, recalling the boundary condition $u(0; \alpha) = 1$, the factor $\sqrt{1 - \alpha u}$ in the differential equation is singular at the origin. Indeed, $u(x; 1)$ does not have a power series about the origin. Let S denote $-u_x(0) \approx 1.3282293391$. Then direct substitution into the differential equation shows that for small x,

$$
u(x) = 1 - Sx + \frac{8}{15}\sqrt{S}x^{5/2} - \frac{8}{45}x^4 + \frac{224}{7,425}\frac{x^{11/2}}{\sqrt{S}} - \frac{64}{155,925}\frac{x^7}{S}
$$

$$
- \frac{39,104}{66,268,125}\frac{x^{17/2}}{S^{3/2}} - \frac{237,568}{14,910,328,125}\frac{x^{10}}{S^2}
$$

$$
+ \frac{40,337,152}{1,760,412,740,625}\frac{x^{23/2}}{S^{5/2}} + \frac{92,444,672}{360,084,424,219,875}\frac{x^{13}}{S^3} + \ldots
$$

$$(13)$$

Maple's **dsolve(...“series”)** fails, but the Maple code in Table 2 suffices to calculate the first 100 terms in a couple of minutes on a laptop.

The coefficients fluctuate with degree in addition to the steady exponential decay, making it difficult to estimate the radius of convergence. However, if the "envelope" of the power series coefficients p_n is bounded by $\exp(-\log(\tilde{\rho})n)$, then the radius of convergence ρ (in $z \equiv x^{3/2}$) is approximately $\rho = \max(\tilde{\rho})$. Alternatively, one can simply plot the partial sums of the series; this will track $u(x)$ up to some finite x and then explode at x equal to the radius of convergence. Both methods give a radius of convergence about 2.5. Padé approximants considerably extend the accuracy of the power series, but we omit the details.

Ironically, the ordinary power series about $x = 0$ for the nonsingular solutions are much less useful than the Puiseaux series for the singular case,
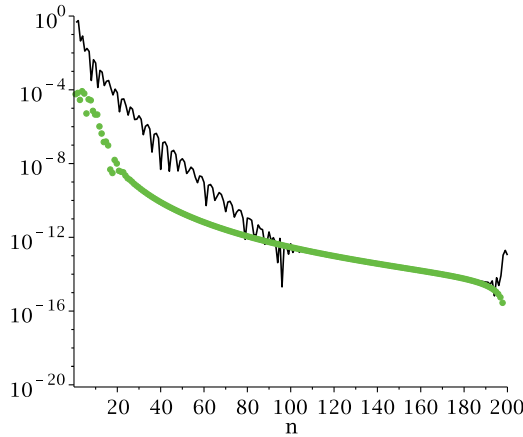
Figure 2. Absolute values of the rational Chebyshev coefficients for $u(x, \alpha = 1)$ [solid black] and for $f_{sing} \equiv (8/15)Sx^{5/2}\exp(-20x)$ where $S = u_x(0, 1) = 1.32822932866$, which was chosen to have the same convergence-limiting singularity as $u(x, \alpha = 1)$. $N = 200$, map parameter $L = 1/2$, and floating point arithmetic with 16 digit precision.

$\alpha = 1$. The power series for general α begins

$$u(x) = 1 - Sx + \frac{1}{3}\frac{S}{\sqrt{1-\alpha}}x^3 - \frac{1}{12}\frac{\alpha S^2}{(1-\alpha)^{3/2}}x^4$$

$$+ \left\{\frac{1}{80}\frac{3\alpha^2 S^3}{(1-\alpha)^{5/2}} + \frac{1}{10}\frac{S}{1-\alpha}\right\}x^5 + \dots$$

Noting that Noor and Mohyud-Din [7] used $A = -S$, there is a disagreement in the sign of $(S/10)(1-\alpha)^{-1}x^5$; our choice was checked by computer algebra.

This shows that the radius of convergence is proportional to $(1-\alpha)$ and therefore is tiny when α is near one.

3.2 Rate of Convergence of rational Chebyshev series for a function with an endpoint singularity

Theory predicts that the $x^{5/2}$ singularity should degrade the exponential convergence typical of rational Chebyshev series to a decay rate for the coefficients a_n proportional to n^{-6} [17]. (This is the same as for a finite interval expansion in Chebyshev polynomials; at a fixed point near $x = 0$, the rational Chebyshev functions converge to Chebyshev polynomials with increasing degree [6].) Figure 2 confirms this prediction by comparing the rational Chebyshev coefficients of $u(x, 1)$ with those of a function that is very different but has a branch point at the origin of exactly the same strength and type as in the Puiseaux series for $u(x; 1)$. For large degree, the rational Chebyshev coefficients for the two functions are the same even though the leading coefficients are very different.

Table 3
Errors in Simple Analytic Approximations to $u(x, 1)$

Approximation	Error in L_∞ Norm
$u_0 + u_1 + u_2$ [Kidder α power series]	0.084
$u_0 \equiv 1 - \text{erf}(x)$	0.046
$u_0 - 0.15724\, x \exp(-2x^2)$	0.0037
$u_0 - (0.15395 + 0.00583\, x)\, x \exp(-2x^2)$	0.0038
$u_0 - (0.212827 - 0.218239\, x + 0.180116\, x^2)$ $x \exp(-2x^2)$	0.00086
$u_0 - (0.195302 - 0.1190703\, x + 0.0120895\, x^2$ $+ 0.0827973\, x^3\,)\, x \exp(-2x^2)$	0.00046

Because the singularity is visible only when the coefficients have fallen to 10^{-12}, the singularity is too weak to prevent the pseudospectral method from returning very accurate answers even for this singular case.

Similar weak singularities arise in other classical nonlinear ODE such as the Lane–Emden equation [12] and Thomas–Fermi equation [13, 4].

3.3 Curve-fitting, I

It is easy to least-squares fit analytic expressions to the Chebyshev numerical solutions. Inspired by the Gaussians and error functions in Kidder's perturbation theory, we tried

$$u(x; \alpha) = \text{erfc}(x) + \exp(-2x^2) x\, P_M, \tag{14}$$

where $P_M(x)$ is a polynomial of degree M. These approximations and others are cataloged for the most difficult case, $\alpha = 1$, in Table 3.

It is noteworthy that Kidder's three-term approximation has double the error of this lowest order curve-fitted approximation. About 90% of the correction to $1 - \text{erf}(x)$ is captured by $-0.15724x \exp(-2x^2)$.

4. Curve-fitting, II: approximations in the form erfc(x + p(x))

In WKB approximations to the solution of linear second-order differential equations, cosines and exponentials and Airy functions are uplifted to approximations of equations with slowly varying coefficients by being given arguments that are nonlinear in the coordinate x. We explored similar possibilities here by writing

$$u(x; \alpha) = \text{erfc}(x + p(x\alpha)) \qquad p(x; \alpha) \equiv -x + \text{inverfc}(u(x; \alpha)). \tag{15}$$
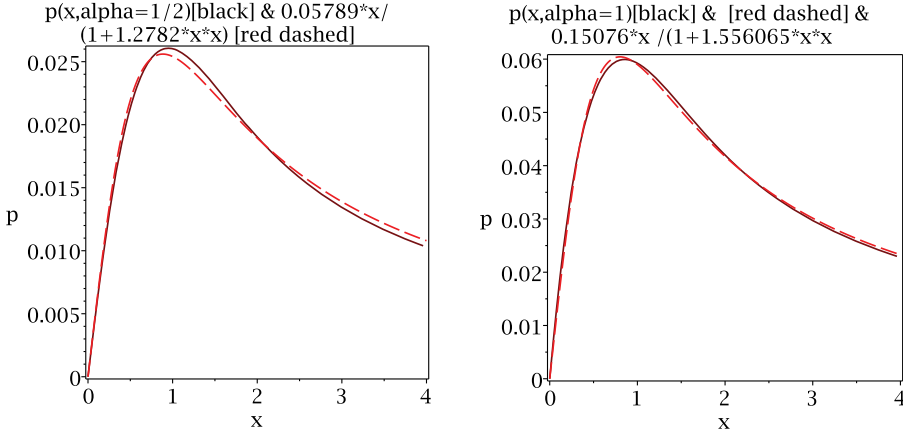
Figure 3. The inside-the-erfc function [solid] compared with rational functions that approximate it [red dashed] for $\alpha = 1/2$ [left] and $\alpha = 1$ [right.]

We then performed a nonlinear curve-fit of a rational approximation to $p(x;\alpha)$ as calculated by the pseudospectral method.

The inverse complementary error function is not widely available in software libraries, but the simple formulas needed can be found in the book [21] and [20, 19, 32].

Figure 3 shows that $p(x;\alpha)$ is very smooth and

$$\max_{x\in[0,\infty]} \left| u(x;1) - \mathrm{erfc}\left(x + \frac{0.15076x}{1 + 1.55607x^2} \right) \right| = 0.0019. \tag{16}$$

An error of less than one part in 500 of the maximum of u is remarkable.

5. Slope at the origin

The spatial derivative of $u(x;\alpha)$ at $x = 0$ has a special significance because if this is known accurately, then the power series about the origin is completely determined and a boundary value problem can be solved numerically as an initial-value problem.

The slope at the origin, the negative of the defined-to-be-positive parameter S in our power series analysis, can be approximated in various ways. Kidder's perturbation theory gives

$$u_x(0) = -S = -\frac{2}{\sqrt{\pi}} \left\{ 1 + \frac{1}{4}\left(1 - \frac{2}{\pi} \right)\alpha \right.$$

$$\left. + \left(-\frac{13}{16} + \frac{1}{2\pi} - \frac{\sqrt{\pi}}{24} + \frac{5}{32}\pi + \frac{3\sqrt{3}}{16} \right)\alpha^2 \right\}. \tag{17}$$

Below we derive a better approximation, through a different perturbation approach, and compute very accurate reference values for the slope using the pseudospectral method.

5.1 Delta-expansion approximation

The presence of a weak algebraic nonlinearity in the Kidder equation suggests that good approximations could be obtained using the delta-expansion method by Bender and coworkers [5]. To this end, we consider a more general problem

$$u'' + 2x(1 - \alpha u)^{\delta} u' = 0 \qquad u(0) = 1, \, u(\infty) = 0, \tag{18}$$

with δ a parameter, which reduces to the Kidder problem for $\delta = -1/2$ (note that in this subsection derivation with respect to x will also be denoted by a prime). Because we know the solution to the problem for $\delta = 0, u = u_o(x) = 1 - \mathrm{erf}(x)$, we may seek the solution, for a generic δ, as the series expansion

$$u(x) = u_0(x) + \delta u_1(x) + \delta^2 u_2(x) + \dots. \tag{19}$$

Placing this expansion in (19), and comparing powers of δ, yields a sequence of linear, homogeneous boundary value problems that can be solved by quadratures. The first two of them are

$$u_1'' + 2x u_1' = -2x F_0 u_0', \qquad\qquad u_1(0) = u_1(\infty) = 0, \tag{20}$$

$$u_2'' + 2x u_2' = -2x F_0 u_1' - x F_0^2 u_0', \qquad u_2(0) = u_2(\infty) = 0, \tag{21}$$

where we have defined

$$F_0(x) \equiv \ln[1 - \alpha u_0(x)]. \tag{22}$$

Integrating once the equation for u_1 gives

$$u_1' = e^{-x^2} \left(C + \frac{4}{\sqrt{\pi}} \int_0^x d\xi \, \xi \, F_0(\xi) \right), \tag{23}$$

with C a constant that, multiplied by δ, determines the first-order term in the expansion for the slope at the origin:

$$u_x(0) = -2/\sqrt{\pi} + C \delta + u_2'(0) \delta^2 + \dots \tag{24}$$

Integrating again, and using the boundary condition at $x = 0$, we get

$$u_1 = C \int_0^x d\xi e^{-\xi^2} + \frac{4}{\sqrt{\pi}} \int_0^x d\xi \, e^{-\xi^2} \int_0^{\xi} d\eta \, \eta \, F_0(\eta) \tag{25}$$

with C that can now be determined by asking that u_1 vanishes at infinity. After an integration by parts of the term with the double integral, we obtain

$$C = -\frac{4}{\sqrt{\pi}} \int_0^{\infty} dx \, u_0(x) F_0(x). \tag{26}$$

Table 4

Errors in Perturbation Theory for the Slope at the Origin

α	Pseudospectral	δ-First Error	$O(\alpha)$ Error	δ-2d Error	$O(\alpha^2)$ Error
0.1	-1.139007206178300	-0.000093	-0.00038	0.000068	-0.00011
0.2	-1.150475486216286	-0.00041	-0.0016	0.00029	-0.00051
0.3	-1.162941458295912	-0.0010	-0.0038	0.00068	-0.0014
0.4	-1.176615666683335	-0.0020	-0.0072	0.0013	-0.0029
0.5	-1.191790649719421	-0.0034	-0.012	0.0021	-0.0054
0.6	-1.208894174540914	-0.0056	-0.019	0.0033	-0.0092
0.7	-1.228598473695921	-0.0087	-0.028	0.0048	-0.015
0.8	-1.252083790143917	-0.014	-0.042	0.0067	-0.024
0.9	-1.281881322203357	-0.022	-0.061	0.0090	-0.039
1.0	-1.32822934	-0.040	-0.097	0.0093	-0.070

Note: The pseudospectral computations were performed multiple times using various precisions, map parameters L, and numbers of basis functions N. All digits shown are believed trustworthy.

Thus, the slope for the Kidder problem to first order is given by

$$u_x(0) = -\frac{2}{\sqrt{\pi}} \left(1 - \int_0^\infty dx\, x\, u_0(x) F_0(x) \right). \tag{27}$$

The second-order calculation is more laborious, but straightforward; we only give here the resulting expression for the slope:

$$\frac{\sqrt{\pi}}{2} u_x(0) = -1 + \int_0^\infty dx\, x\, u_0(x) F_0(x) - \left(\int_0^\infty dx\, x\, u_0(x) F_0(x) \right)^2 \tag{28}$$

$$-\frac{1}{4} \int_0^\infty dx\, x\, u_0(x) F_0^2(x) + \int_0^\infty dx\, x\, u_0(x) F_0(x) \int_0^x d\xi\, \xi\, F_0(\xi).$$

In Table 4 and Figure 4, the first-order and second-order approximations for $u_x(0)$ we have derived are compared with the corresponding results from the expansion in α, Equation (17), using the pseudospectral calculation as a reference. The results from the delta-expansion approach are significantly more accurate than the latter at both orders.

5.2 Chebyshev approximations

It is trivial to expand the slope at the origin as a Chebyshev polynomial series merely by evaluating $du/dx(x;\alpha)$ at the discrete parameter values

$$\alpha_j = \frac{1}{2} \left\{ 1 + \cos\left(\pi\, \frac{(2j-1)}{2M} \right) \right\}, \qquad j = 1, 2, \ldots M \tag{29}$$
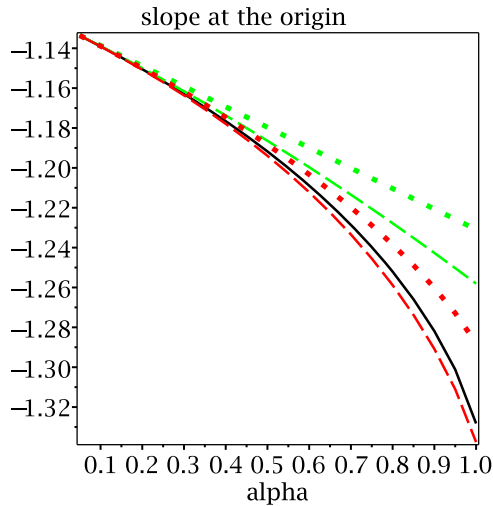
Figure 4. Slope at the origin versus the parameter α. The exact values are the solid black curve. The dotted curves are the first-order Kidder (α-power series, green) and delta-expansion (red). The green and red dashed lines are the α and delta series at second order. At both orders, the delta-expansion is much more accurate than the power series in α.

and then calculating the M-point Chebyshev interpolant through a matrix vector multiplication or a Fast Cosine Transform [10].

The Chebyshev coefficients in the ensuing approximation,

$$\frac{du}{dx}(0;\alpha) \approx \sum_{n=0}^{M-1} b_n T_n(2\alpha - 1), \qquad \alpha \in [0, 1] \tag{30}$$

are very closely approximated by $b_n \sim -1/n^4$ as shown in Figure 5.

This fourth-order rate of convergence (and also the fact that the coefficients are all of the same sign) implies that $du/dx(0;\alpha)$ has the same three-halves power singularity at $\alpha = 1$ as $du/dx(x;1)$ has at $x = 0$ for $\alpha = 1$. (Note that u itself has a weaker five-haves singularity and sixth order Chebyshev convergence as discussed n Sec. 3.2.)

The pernicious effects of such singularities can be greatly diminished by a change of coordinate. However, the singularity is usually only weakened but not eliminated unless the mapping is exponential near the singularity, which can lead to lamentably large condition numbers and round-off difficulties. Furthermore, the lowest few coefficients in the transformed series often converge at a lower rate than the untransformed series and only at a finite "crossover degree" do the transformed coefficients dip below those of the original series [7].
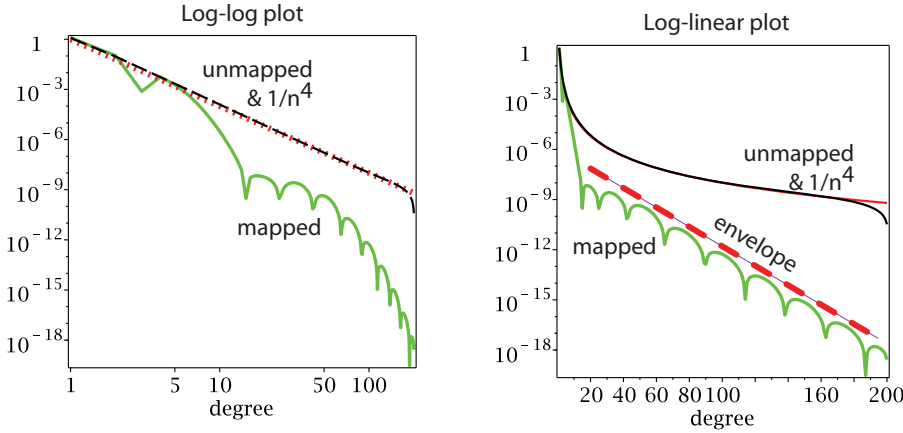
Figure 5. Chebyshev coefficients of the expansion of $du/dx(0, \alpha)$ on $\alpha \in [0, 1]$ using a standard Chebyshev interpolant [upper curves, black] and the same with use of the transformation described in the text [lower curves, green]. The power law $1/n^4$ is shown as a thin, dotted red curve in both panels, but is graphically indistinguishable from the unmapped coefficients. The panels are identical except that degree n is on a logarithmic scale on the left and a linear scale on the right. The mapped coefficients oscillate, but are tightly bounded by a straight line ("envelope of the Chebyshev coefficients") on the log-linear plot, showing a geometric rate of convergence. Slopes were calculated in 32-digit arithmetic using a basis of 100 rational Chebyshev functions with $L = 1$.

Here, however, a simple sine map is completely successful. The pseudospectral rational Chebyshev code is applied to compute the slope at

$$\alpha_j = \sin\left(\frac{\pi}{4}\left\{1 + \cos\left(\pi\,\frac{(2j-1)}{2M}\right)\right\}\right), \qquad j = 1, 2, \dots M. \qquad (31)$$

This is equivalent to expanding

$$\frac{du}{dx}(0; \alpha) \approx \sum_{n=0}^{M-1} b_n^{map} T_n\left(\frac{4}{\pi}\arcsin(\alpha) - 1\right), \qquad \alpha \in [0, 1]. \qquad (32)$$

It is often simplest to use the identity $T_n(\cos(t)) = \cos(nt)$ and evaluate the Chebyshev series as a cosine series:

$$\frac{du}{dx}(0; \alpha) \approx \sum_{n=0}^{M-1} b_n^{map} \cos(nt[\alpha]), \qquad (33)$$

$$t(\alpha) = \arccos\left(\frac{4}{\pi}\arcsin(\alpha) - 1\right). \qquad (34)$$

Table 5 compares the mapped and unmapped coefficients. The absolute error in a Chebyshev series is bounded by the sum of the absolute values of the

Table 5

Chebyshev Coefficients for the Expansion of the Slope at the Origin

n	$b_n[Unmapped]$	b_n^{map}	$\sum_{m=n+1}^{\infty} |b_m^{map}|$
0	−1.21	−1.231156749	0.115
1	−0.93e-1	−0.1060222204	0.895e-2
2	−0.18e-1	0.7559800182e-3	0.820e-2
3	−0.54e-2	0.5491086172e-2	0.270e-2
4	−0.22e-2	0.1931853685e-2	0.772e-3
5	−0.10e-2	0.5622806751e-3	0.210e-3
6	−0.54e-3	0.1533651140e-3	0.566e-4
7	−0.31e-3	0.4119750581e-4	0.154e-4
8	−0.19e-3	0.1108573988e-4	0.433e-5
9	−0.12e-3	0.2980013212e-5	0.135e-5
10	−0.83e-4	0.7660439328e-6	0.586e-6
11	−0.55e-4	0.1522246725e-6	0.434e-6
12	−0.41e-4	-0.1505159380e-7	0.419e-6
13	−0.30e-4	-0.5229794399e-7	0.367e-6
14	−0.23e-4	-0.4957522833e-7	0.317e-6
15	−0.17e-4	-0.3440774427e-7	0.283e-6
16	−0.13e-4	-0.1641497670e-7	0.266e-6
17	−0.10e-4	0.3707242865e-9	0.266e-6
18	−0.86e-5	0.1404289584e-7	0.252e-6
19	−0.69e-5	0.2378556137e-7	0.228e-6
20	−0.57e-5	0.2948507719e-7	0.198e-6

neglected higher coefficients; this bound on truncation up to and including b_n is shown as the rightmost column.

Power laws are linear on a graph with both vertical and horizontal logarithmic scales and geometric convergence is linear on a graph with a logarithmic vertical scale and linear horizontal scale. In Figure 5, the log–log plot [left] shows that the Chebyshev coefficients of $du(0; \alpha)/dx$ indeed converge at a fourth-order rate. The log-linear plot shows that the mapped coefficients are bounded by a straight line ("envelope") proportional to roughly $\exp(-n/8)$.

The mapping is quadratic near $\alpha = 1$, that is, the mapping $z = (4/\pi)\arcsin(\alpha) - 1$ where $z \in [-1, 1]$ is the Chebyshev argument gives

$$1 - \alpha \approx \frac{\pi^2}{32}(z - 1)^2 + O([z - 1]^4). \qquad (35)$$

Table 6

Values of $S(\alpha)$ from the Padé Approach Using erf(x) as the Independent Variable

α	Pseudospectral	$Eq.(46)$
0.1	1.1390072	1.1387134
0.2	1.1504755	1.1501254
0.3	1.1629415	1.1627908
0.4	1.1766157	1.1769121
0.5	1.1917906	1.1927055
0.6	1.2088942	1.2103471
0.7	1.2285985	1.2297778
0.8	1.2520838	1.2499364
0.9	1.2818813	1.2646350
1.0	1.3282293	1.1283792

Thus, $(1 - \alpha)^{3/2}$ becomes $(z - 1)^3$ near the endpoint $z = 1$, but the cube is not singular. The mapping has *destroyed* the *singularity*.

Note that in view of the logarithmic singularities also lurking in the Kidder equation, it was far from obvious *a priori* that the mapping would work so well.

6. A heuristic explanation for why $u(x, \alpha)$ differs so little from erfc(x)

Define $v(x; \alpha) \equiv u_x(x; \alpha)$. Without approximation,

$$v_x + q(x; \alpha)v = 0, \qquad v(x, 0) = -S \exp\left(- \int_0^x q(y; \alpha)dy\right), \qquad (36)$$

$$q(x; \alpha) \equiv \frac{2x}{\sqrt{1 - \alpha u(x; \alpha)}}. \qquad (37)$$

When $\alpha = 0$, $q(x; \alpha) = 2x$ whose integral is x^2 and thus $v(x; 0) = -S \exp(-x^2)$. When $\alpha = 1$, the denominator is not everywhere one, but instead has a square root singularity at $x = 0$ where the denominator vanishes. Why, then, does $u(x; 1)$ differ from $u(x; 0)$ by less than 0.046?

The answer is that the denominator of $q(x; \alpha)$ differs from one only near the origin where the *numerator* is small, too. Figure 6 shows that the coefficient $q(x; \alpha)$ does not vary greatly with α. The relative insensitivity of this coefficient of the differential equation translates to a similar insensitivity to the parameter α in $u(x; \alpha)$ itself.
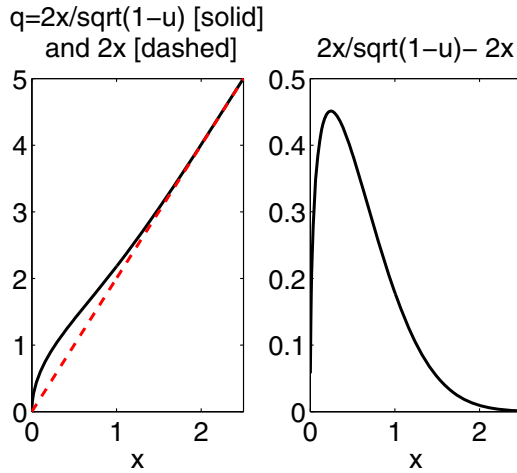
Figure 6. (Left) The solid black curve is $q(x; \alpha) \equiv 2x/\sqrt{1 - \alpha u(x; \alpha)}$ for the extreme case of $\alpha = 1$ and where $u(x; \alpha)$ was approximated by $u(x; 1) \approx 1 - \text{erf}(x)$. The dashed curve is $q(x; \alpha = 0) = 2x$. (Right) $q(x; \alpha = 1) - q(x; \alpha = 0)$.

7. Padé approximants

Padé approximants provide a simple way for extending the accuracy of the series expansions about the origin beyond their range of convergence. They have been used for the Kidder problem in [34] and [26], with awful results (see, e.g., table 6.1 of [26]): the accuracy of $S(\alpha)$ is poor for $\alpha = 0.5$, and further deteriorates at smaller and larger values of α, because, against all the available numerical and analytical evidence, S is found to be a *decreasing* function of α. It is interesting to look at the reasons for this failure.

In the cited works, the series expansion of $u(x)$ is used to construct low-order approximants; in particular, the (2, 2) and (3, 3) diagonal Padé's, which are ratios of polynomials of second and third degrees, respectively. Being derived from the series, the coefficients of the polynomials depend on S, so the accuracy of the approximants depends on how accurately one can determine S using some additional constraint. A seemingly reasonable approach is "Padé-shooting," which is to impose the boundary condition on u at infinity, setting to zero the coefficient of the highest order term in the numerator of the Padé rational approximation. This was pioneered for general nonlinear ODEs by Fernandez [18] and Boyd [8]. It was applied to the Kidder equation in [34] and [26], but the resulting expressions for $S(\alpha)$ are terribly inaccurate. This just shows that the low-order Padé's in consideration cannot capture the large-x behavior of the solution to the Kidder problem, which is characterized by a fast, nonalgebraic decay (u_x approximately decays as e^{-x^2} at large x). It also suggests that better rational approximations could be obtained by first introducing a new

independent variable that incorporates the exponential decay. A natural choice is

$$z \equiv \frac{2}{\sqrt{\pi}} \int_0^x d\xi \, e^{-\xi^2} = \text{erf}(x), \qquad (38)$$

which yields

$$u_x = \frac{2}{\sqrt{\pi}} e^{-x^2} u_z. \qquad (39)$$

The function $u(z)$ is defined over $[0, 1]$, and vanishes for $z = 1$. Its derivative at the origin is given by

$$u_z(0) = \frac{\sqrt{\pi}}{2} u_x(0) \equiv -\tilde{S}, \qquad (40)$$

where $\tilde{S}$ is the S parameter, scaled by its value for $\alpha = 0$ $[\tilde{S}(0) = 1]$. Computing higher order derivatives, we obtain the following series expansion for $u(z)$ about the origin:

$$u(z) = 1 - \tilde{S} z + A \tilde{S} z^3 - B \tilde{S}^2 z^4 + ..., \qquad (41)$$

with

$$A \equiv \frac{\pi}{12} \left[\frac{1}{(1 - \alpha)^{1/2}} - 1 \right], \qquad B \equiv \frac{\pi}{48} \frac{\alpha}{(1 - \alpha)^{3/2}}. \qquad (42)$$

The terms up to z^3 in the expansion are sufficient to compute the $(2, 2)$ Padé

$$u(z) = \frac{(1 - z)[1 + az]}{1 + bz + cz^2}, \qquad (43)$$

where

$$a = \frac{A}{\tilde{S} - 1} - S, \qquad b = \frac{A}{\tilde{S} - 1} - 1, \qquad c = A. \qquad (44)$$

Then, to determine $\tilde{S}$, we can go to next order, and equate the coefficient of the z^4 term in (41) with the corresponding term in the expansion of the approximant. This yields a quadratic equation for $\tilde{S}$,

$$\tilde{S}^2 + \left(\frac{A}{B} - 1 \right) \tilde{S} - \frac{A}{B}(A + 1) = 0. \qquad (45)$$

with the meaningful (positive) root given by

$$\tilde{S} = \frac{1}{2} \left[-\left(\frac{A}{B} - 1 \right) + \sqrt{\left(\frac{A}{B} - 1 \right)^2 + 4 \frac{A}{B}(A + 1)} \right]. \qquad (46)$$

As shown in Table 6, this expression gives accurate values for the slope up to $\alpha \simeq 0.8$ (the corresponding profiles, computed from the Padé (43),

are also accurate). Then accuracy is lost, because of the shrinking of the convergence range of the series expansion for $\alpha \to 1$. In any case, the change of independent variable has allowed for a tremendous improvement on the results of [34] and [26].

8. Connection with the Blasius function

The similarity solution for the idealized flow of a viscous fluid past an infinitesimally thick, semi-infinite flat plate is the Blasius function $f(x)$. A thorough discussion is given in [11, 9]. Boyd [11] provides a table of coefficients in a rational Chebyshev series which can be used to compute the Blasius function and its derivatives to about 15 decimal places. Because the Blasius function is parameter-free, the tabulated coefficients are mere numbers, not functions of a parameter. Remarkably, the Blasius function can be used to evaluate the limiting solution to Kidder's equation as expressed by the following.

THEOREM 1 Blasius–Kidder connection. *Define the Blasius function as the solution to*

$$2f_{\eta\eta\eta} + ff_{\eta\eta} = 0, \qquad \eta \in [0, \infty] \tag{47}$$

subject to $f(0) = f_\eta(0) = 0$, $f_\eta(\infty) = 1$. *Let* $u(x; \alpha = 1)$ *denote the solution to the Kidder equation.*
  Then

$$u(x; \alpha = 1) = 1 - \left(f_\eta(2f^{-1}(x))\right)^2, \tag{48}$$

where $f^{-1}(x)$ *is the inverse of the Blasius function, that is, the equation* $f(\eta) = x$ *is solved by* $\eta = f^{-1}(x)$.

  Proof: Writing

$$f_\eta(\eta) = X(f), \tag{49}$$

transforms the Blasius equation into the second-order problem

$$XX_{ff} + X_f^2 + (1/2)fX_f = 0; \qquad X(0) = 0, \ X(\infty) = 1. \tag{50}$$

On the other hand, writing

$$2x = \tilde{x}, \qquad u(\tilde{x}) = 1 - Y^2, \tag{51}$$

transforms the Kidder equation into

$$YY_{\tilde{x}\tilde{x}} + Y_{\tilde{x}}^2 + (1/2)\tilde{x}Y_{\tilde{x}} = 0; \qquad Y(0) = (1 - \alpha)^{1/2}, \ Y(\infty) = 1. \tag{52}$$

Clearly, the boundary value problems for X and Y exactly coincide for $\alpha = 1$. Thus, for this limiting value,

$$Y(\tilde{x}) = X(f), \tag{53}$$

Together with the definitions of X, Y, and $\tilde{x}$, this implies (48), thus completing the proof.

We have also checked (48) numerically. The Blasius function was inverted by solving $f(\eta) = x$ using Newton's iteration

$$\eta^{(n+1)} = \eta^{(n)} - \frac{f(\eta^{(n)}) - x}{f_\eta(\eta^{(n)})}. \tag{54}$$

A Never-Failing Newton's Initialization [14], derived from power series and asymptotic approximations to the Blasius function, is

$$\eta^{(0)} = \begin{cases} 2.45 + \sqrt{x}, & x < 2 \\ x + 1.72, & x \geq 2. \end{cases} \tag{55}$$

9. Summary

The study reported here and the works we cite have made the Kidder function $u(x; \alpha)$ a noncanonical special function. "Noncanonical" in that it does not appear in either the *NBS Handbook of Mathematical Functions* [2] or its successor, the *NIST Digital Library* [27]. "Special function" in that the catalog of properties, expansions, and approximations is now as extensive as for many of the canonical functions.

This function is a good classroom example for classes in numerical analysis. The numerical subtlety is that although $u(x; \alpha)$ is singular at $\alpha = 1$ and singular as a function of x near the left endpoint for α near one, blind application of Chebyshev pseudospectral methods yields 12 decimal place accuracy and apparent geometric convergence! When a singularity is weak in the sense that only a high-order derivative is infinite, and the singularity is at an endpoint, it may be ignorable for practical purposes. Singularity-induced degradation of the convergence rate from exponential to a power law in degree n does appear for the Kidder problem, but only at very high degree. The standard remedy for branch points on or near the expansion interval is to use a change-of-coordinate. Although not really needed here, a simple sine mapping restores geometric convergence.

The Kidder problem is also a good example for classes in perturbation methods. It is possible to explicitly extend both Kidder's power series in α [the obvious perturbation parameter] and the delta-expansion [in which the perturbation parameter is the nonlinearity exponent] to second order. The delta expansion is much superior. An approximation which is a quadratic polynomial in an exponentially mapped coordinate $z(x)$ divided by another quadratic polynomial in the same variable gives estimates of the slope at the origin accurate to one part in 4000 for $\alpha = 0.4$ and to one part in 400 for $\alpha = 0.8$, a vast improvement on the analogous results from the α power series. The

superiority of the delta-expansion is another piece of evidence that nonobvious choices of perturbation parameter can be very effective [5, 36, 37].

Finally, the Kidder problem is an illustration of the duality that is seen in many other classic problems such as the Blasius flow. On the one hand, the ODE is hard because it is a nonlinear boundary value problem with an unbounded domain, singularities and near-singularities, and no explicit solution is known. On the other, the function is smooth, never deviating more than 0.05 from the complementary error function over its entire parameter range, well-approximated by remarkably simple expressions.

One is reminded of the old joke about the Cambridge mathematician who became stuck in the middle of a classroom demonstration he had described at the beginning as obvious, disappeared into his adjoining office to calculate furiously for half an hour, and finally returned just before the end of the class to inform the students, "Oh, yes, it's really obvious!"

We hope our contributions have made the Kidder problem a little more obvious.

Acknowledgment

References

1. S. ABBASBANDY, Numerical study on gas flow through a micro-nano porous media, *Acta Phys. Pol.* 121:581–585 (2012).
2. M. ABRAMOWITZ and I. A. STEGUN, *Handbook of Mathematical Functions*, Dover, New York, 1965.
3. R. P. AGARWAL and D. O'REGAN, Infinite interval problems modeling the flow of a gas through a semi-infinite porous medium, *Stud. Appl. Math.* 108:245–257 (2002).
4. P. AMORE, J. P. BOYD, and F. M. FERNANDEZ, Accurate calculation of the solutions to the Thomas–Fermi equations, *Appl. Math. Comput.* 232:929–943 (2014).
5. C. M. BENDER, K. A. MILTON, S. S. PINSKY, and L. M. SIMMONS, Jr., A new perturbative approach to nonlinear problems, *J. Math. Phys.* 30:1447–1455 (1989).
6. J. P. BOYD, Orthogonal rational functions on a semi-infinite interval, *J. Comput. Phys.* 70:63–88 (1987).
7. J. P. BOYD, The asymptotic Chebyshev coefficients for functions with logarithmic endpoint singularities, *Appl. Math. Comput.* 29:49–67 (1989).
8. J. P. BOYD, Padé approximant algorithm for solving nonlinear ODE boundary value broblems on an unbounded domain, *Comput. Phys.* 11:299–303 (1997).
9. J. P. BOYD, The Blasius function in the complex plane, *J. Experimental Math.* 8:381–394 (1999).
10. J. P. BOYD, *Chebyshev and Fourier Spectral Methods* (2nd ed.), Dover, Mineola, New York, 2001, 665 pp.

11. J. P. BOYD, The Blasius function: computations before computers, the value of tricks, undergraduate projects, and open research problems, *SIAM Rev*. 50:791–804 (2008).

12. J. P. BOYD, Chebyshev spectral methods and the Lane–Emden problem, *Numer. Math Theor. Appl*. 4:142–157 (2010).

13. J. P. BOYD, Rational Chebyshev series for the Thomas–Fermi function: endpoint singularities and spectral methods, *J. Comput. Appl. Math*. 231:90–101 (2013).

14. J. P. BOYD, *Solving Transcendental Equations: The Chebyshev Polynomial Proxy and Other Numerical Rootfinders, Perturbation Series and Oracles*, SIAM, Philadelphia, 2014, 490 pp.

15. M. COUNTRYMAN and R. KANNAN, Nonlinear boundary value problems on semi-infinite intervals, *Comput. Math. Appl*. 28:59–75 (1994).

16. H. T. DAVIS, *Introduction to Nonlinear Differential and Integral Equations*, Dover Publications, New York, 1962, 560 pp; Kidder Eq. on pgs. 410–411. The 1960 edition, published by a government agency and therefore in the public domain, is available online.

17. H. EISEN and W. HEINRICHS, A new method of stabilization for singular perturbation problems with spectral methods, *SIAM J. Numer. Anal*. 29:107–122 (1992).

18. F. M. FERNANDEZ, Strong coupling expansion for anharmonic oscillators and perturbed Coulomb potentials, *Phys. Lett. A* 166:173–176 (1992).

19. H. E. FETTIS, Corrigendum: "a stable algorithm for computing the inverse error function in the "tail-end" region," *Math. Comput*. 29:673 (1974).

20. H. E. FETTIS, A stable algorithm for computing the inverse error function in the "tail-end" region, *Math. Comput*. 28:585–587 (1974).

21. A. GIL, J. SEGURA, and N. TEMME, *Numerical Methods for Special Functions*, SIAM, Philadelphia, 2007.

22. W. HEINRICHS, Improved condition number for spectral methods, *Math. Comput*. 53:103–119 (1989).

23. Y. KHAN, N. FARAZ, and A. YILDIRIM, Series solution for unsteady gas equation via MLDM-Pade technique, *World Appl. Sci. J*. 9:27–31 (2010).

24. R. E. KIDDER, Unsteady flow of gas through a porous medium, *J. Appl. Mech*. 24:329–332 (1957).

25. M. MALEKI, I. HASHIM, and S. ABBASBANDY, Analysis of IVPs and BVPs on semi-infinite domains via collocation methods, *J. Appl. Math*. (2010), article ID 696574.

26. M. A. NOOR and S. T. MOHYUD-DIN, Variational iteration method for unsteady flow of gas through a porous medium using He's polynomials and Pade approximants, *Comput. Math. Appl*. 58:2182–2189 (2009).

27. F. W. J. OLVER, D. W. LOZIER, R. F. BOISVERT, and C. W. CLARK, eds., *NIST Handbook of Mathematical Functions*, Cambridge University Press, New York, 2010.

28. K. PARAND, M. SHAHINI, and A. TAGHAVI, Generalized Laguerre polynomials and rational Chebyshev collocation method for solving unsteady gas equation, *Int. J. Contemp. Math. Sci*. 4:1005–1011 (2009).

29. K. PARAND, A. TAGHAVI, and M. SHAHINI, Comparison between rational Chebyshev and modified generalized Laguerre functions pseudospectral methods for solving Lane–Emden and unsteady gas equations, *Acta Phys. Pol. B* 40:1749 (2009).

30. A. R. REZAEI, K. PARAND, and A. PIRKHEDRI, Numerical study on gas flow through a micro-nano porous media based on special functions, *J. Comput. Theor. Nanosci*. 8:282–288 (2011).

31. R. E. ROBSON and A. PRYTZ, The discrete ordinate/pseudo-spectral method: review and application from a physicist's perspective, *Aust. J. Phys*. 46:465–495 (1993).

32. A. J. STRECOK, On the calculation of the inverse of the error function, *Math. Comput*. 22:14–158 (1968).

33. A. Taghavi, K. Parand, and H. Fani, *Int. J. Comput. Math. Sci*. 3:40– (2009).
34. A.-M. Wazwaz, The modified decomposition method applied to unsteady flow of gas through a porous medium, *Appl. Math. Comput*. 118:123–132 (2001).
35. A.-M. Wazwaz, The variational iteration method for solving linear and nonlinear odes and scientific models with variable coefficients, *Cent. Eur. J. Eng*. 4:64–71 (2014).
36. K. G. Wilson and M. E. Fisher, Critical exponents in 3.99 dimensions, *Phys. Rev. Lett*. 28:240–243 (1972).
37. E. Witten, Quarks, atoms, and the $1/n$ expansion, *Phys. Today* 33:38–43 (1980).